

Underwater Laser Scanning: Integration and Testing in different environments

Annika L. WALTER, Ellen HEFFNER, Annette SCHEIDER and Harald STERNBERG, Germany

Key words: Optical hydrography, Underwater Laser Scanner, System Integration, Test Environments, Resolution

SUMMARY

With the global expansion of underwater infrastructure elements such as port facilities, offshore wind turbines, pipelines and submarine cables, the demand for a fast, precise and high-resolution monitoring solution is growing. While acoustic systems like echosounders only offer a low accuracy in the range of centimetre, passive optical technologies such as cameras depend on illumination, which limits their application particular in deep sea environments. In contrast, active optical LiDAR technologies, known for their superior speed and accuracy, offer a promising alternative. Nevertheless, water also introduces challenges for active optical systems, including turbidity as well as a limited range. The underwater laser scanner ULi, developed by the Fraunhofer IPM, aims to address these limitations. To assess whether the technical specifications provided by the manufacturer, especially with regard to the achievable resolution can be meet, various tests in a basin with clear water are carried out. By using targets consisting of different materials and surface characteristics, a first statement to which extend ULi is suitable for practical underwater monitoring applications, can be made. It can be concluded, that (1) light, shiny and smooth surfaces are less subject to scattering than dark, matt and rough surfaces, (2) the shape of the target does not significantly influence the quality of the derived point cloud and that (3) structures with a size in the range of millimetres can be detected in the near field.

Underwater Laser Scanning: Integration and Testing in different environments

Annika L. WALTER, Ellen HEFFNER, Annette SCHEIDER and Harald STERNBERG, Germany

1. MOTIVATION AND INTRODUCTION

The development of laser scanners marks a significant milestone in advancing geodetic measuring instruments, enabling the transition from discrete to continuous measurements and facilitating the capture of entire objects instead of isolated points [Witte & Sparla, 2015]. Deployed on airborne and land-based platforms, laser scanners can acquire large volumes of 3D data with exceptional accuracy, resolution and speed, making them essential for geospatial information gathering [Shan & Toth, 2018]. Applications range from the creation of digital terrain and city models to forest management as well as the documentation of cultural heritage sites [Vosselman & Maas, 2010].

Driven by the enormous potential that laser scanning systems already deliver on the landsite, the interest in capturing respective 3D data also in aquatic environments, continuously increases [Hildebrandt et al., 2008]. Hereby, laser scanners are of particular interest in the scope of underwater infrastructure elements including for instance port facilities, offshore wind turbines, pipelines, submarine cables and drilling platforms, which all require regular inspection, maintenance and repair operations [Nauert & Kampmann, 2023]. Driven by the potential to operate terrestrial laser scanners on water-based platforms such as vessels or unmanned vehicles, the development of underwater laser scanners was strongly driven forward in the past years. One example for a recently developed system is the underwater light detection and ranging system (ULi), which was developed by the Fraunhofer IPM in Germany and purchased by the HafenCity University Hamburg. A perspective idea of how this particular system can be used for future operations, such as the inspection of underwater pipelines by mounting it on a remotely or an autonomous underwater vehicle, is illustrated in the Figure 1 below.

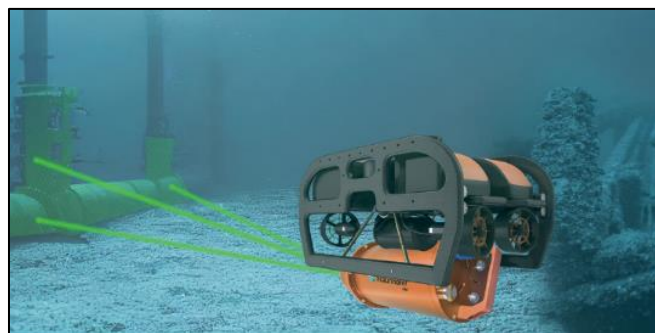


Fig. 1: Conceptual application of ULi [Fraunhofer IPM, 2024]

2. SENSOR TECHNOLOGY

The underwater laser scanner ULi consists of two major components, being a housing, which contains the actual scanning unit, as well as a processing unit which is used for the sake of steering the data acquisition and accessing the recorded data.

2.1 Housing

The waterproof cylindrical housing, illustrated in the Figure 2 below, has a diameter of 0.172 m, a length of 0.375 m and can be used in depths of up to 300 m. To project the laser beam onto the underwater environment and detect the returning light, a green laser with a wavelength of 532 nm and two rotating wedge prisms, allowing for a 44 ° field of view, are used. While the laser has a pulse repetition rate of 100 kHz, the rotating prisms allow the entire field of view to be captured without moving the underwater laser scanner. The laser pattern can either be set to linear, circular or planar and thus dynamically adapted to the respective field of application [Fraunhofer IPM, 2024].



Fig. 2: Housing of ULi [Fraunhofer IPM, 2024]

2.2 Processing Unit

To supply the scanner with 24 V-DC power and transmit the collected data, a 20 m long cable, which connects the housing of the underwater laser scanner with the backside of the associated processing unit, is used. The processing unit itself is custom designed for rack mounting. Hence, it has a width of 19 inch, a depth of 28.5 cm and a height of 2U rack units. As it can be seen in the Figure 3 [top] below, the backside consists of four cable connection inputs, being from left to right an input for a pressure sensor cable, a 24 V-DC power supply input cable, an ethernet cable and the cable which is connected to the housing of the sensor. The in Figure 3 [bottom] illustrated frontside contains a pressure switch, a lock to start the scanner in the 3B mode, a laser-on-lamp indicating whenever the laser is used in the 3B laser mode and a power on / off switch. Hence, the laser scanner can be operated in two different laser modes, being laser class 2M and 3B. Since the laser radiation from the laser class 3B is dangerous for the human eyes

and skin, an additional pressure sensor is attached to the underwater laser scanner. Consequently, the laser operation in the 3B mode automatically switches off if the water level rises above a certain water pressure level threshold. This significantly enhances the safety at work.



Fig. 3: Processing Unit of ULi Backside [top] and Frontside [bottom]

By connecting the processing unit with the mentioned ethernet cable to a PC or laptop, the entire operation and data acquisition of the underwater laser scanner can be steered over a graphical user interface (GUI). The GUI indicates the status of the scanning system and allows the user to set different parameters including the pulse rate and the laser pattern. Furthermore, the interface is used to start, record and stop the measurement.

2.3 Technical Specifications

With a sampling frequency of up to 100.000 points per second, the system is able to reach a precision in the range of millimetres while offering a measurement range of several tens of meters. Nevertheless, the achievable precision and range strongly depend on the quality of the water body in which the measurements are carried out. While clear waters offer a submillimetre precision and several tens of meters scanning range, turbid waters only allow for a measurement range of two times the secchi depth. Overall, the underwater laser scanner can either be operated statically or dynamically. For a dynamic scenario, the laser scanner can be mounted on a vessel or also on underwater platforms such as remotely operated vehicles [Fraunhofer IPM, 2024].

3. TEST ENVIRONMENT

Since the achievable measurement range and the accuracy depend on the quality of the water, the first test measurements are carried out under laboratory conditions and thus in a clear water

environment. In order to do so, a basin with a length of 1.2 m, a width of 0.6 m and a depth of 0.6 m is used. The corpus of the basin, which is also shown in the Figure 4 below, is made out of acryl glass with a thickness of 12 mm on the short sides and 15 mm on the long sides as well as on the ground glass. To conduct the test measurements, the basin is filled with water from the tab to a water level of 0.454 m. The underwater laser scanner is placed at one end of the basin, allowing for a maximum possible distance between the lenses and the opposite end of the basin.

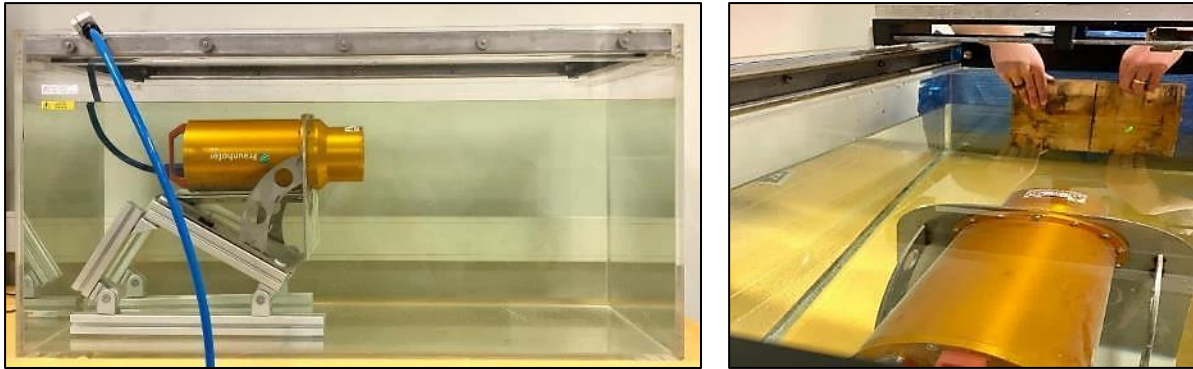


Fig. 4: Test basin with ULi [left] and green laser pointing on wood target pressed onto the acrylic glass [right]

To ensure a horizontal radiation of the measuring laser and thus a good impact angle on the target, a triangular substructure using aluminium construction profiles is established. Using this set-up, which is also shown in the Figure 4 [left], the distance between the lenses and the end of the basin is approximately 0.560 m. While small targets are directly pressed onto the acrylic glass on the end of the basin, as shown in the Figure 4 [right], targets exceeding the height of the basin are held approximately 5 cm in front of the glass rear panel.

4. TARGETS

To assess the suitability of the underwater laser scanner with respect to different tasks, including inspection, maintenance and repair operations of different infrastructure elements, a variety of targets with varying surface characteristics is taken into consideration. An overview of the selected targets is shown in the Figure 5 below. To get a first idea of how the surface texture influences the reflectivity of the green laser, a square black target, shown in the lower right corner of the Figure 5, is used. The target, being a black smooth acrylic plate, is shiny on the one side and foiled on the other side. Subsequently the target can be used to assess in which way shiny and matt appearances influence the reflectivity behaviour of the transmitted laser. To further investigate the impact of the surface roughness, a large white matt acrylic target is used. While one side of the target plate is smooth, the other side is roughened with the help of sandpaper. Following, different metal plates, including steel, coated steel, lacquered steel, rusted steel, brass, copper or aluminium are used for further investigations. When selecting

these materials, care was taken to ensure that they are actually used for the construction of underwater infrastructure elements. Subsequently, steel, whether it is coated or not, is used for the construction of pipelines or quay walls, as well as to establish the fundament of offshore wind turbines or oil drilling platforms. By using an additional rusted steel plate, having a rougher surface in comparison to the lacquered steel plates, the opportunity to use the underwater laser scanner for inspection and maintenance operations on rusted quay walls, being an important topic especially in harbour environments, can be elicited. Furthermore, two targets made out of wood, used in former times for the construction of quay walls or still nowadays in the scope of mooring dolphins, are used.

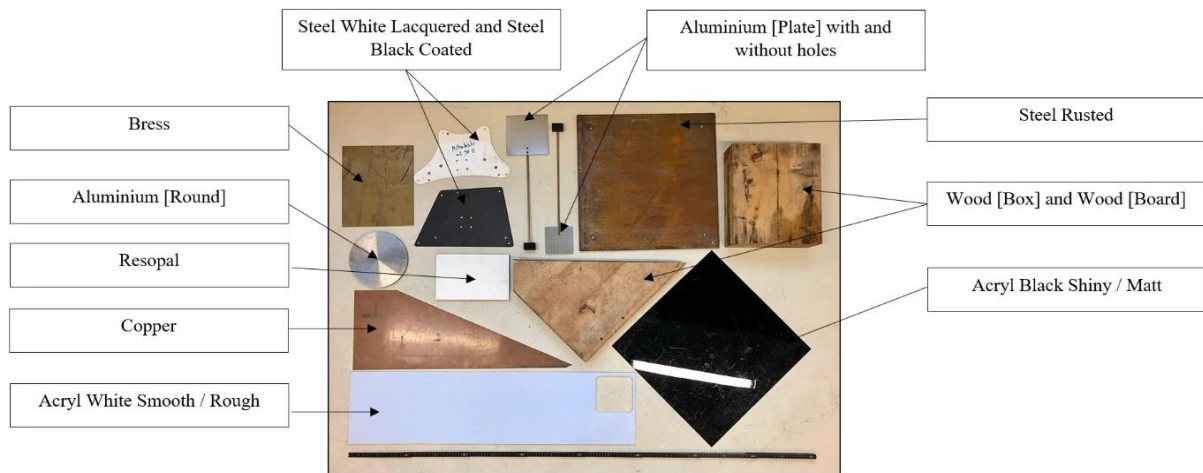


Fig. 5: Used Targets

To get an information on how well the reflective behaviour is with regard to different surface characteristics and to assess whether the underwater laser scanner can be used to detect deformations in the range of millimetres, the existing cracks, holes, scratches et cetera of the tested materials are evaluated. Subsequently, the white lacquered steel plate shown on the top of the Figure 5, the black coated steel plate directly below it, the large rusted steel plate further to the right, the round aluminium target as well as the wood target placed in the centre, all contain man-made drilled holes in various sizes. In addition, another rectangular aluminium target, which has a machine-generated regular hole grid consisting of 12 columns and 11 rows, is used. Subsequently the differently sized holes are used to assess the order of magnitude at which the underwater laser scanner is still able to detect those structures.

5. DATA ACQUISITION

Before the actual test measurements are carried out, the characteristics of the water within the test basin are numerically quantified. Therefore, the multi-sensor oceanographic profiler AML-3 from AML Oceanographic is used. The derived values are summarized in the Table 1. Subsequently, an average turbidity of 0.00 NTU is measured. Since the basin is filled with water

from the tap, a turbidity of 0.00 NTU is expected and the influence of turbidity is therewith eliminated. Hence, the underwater laser scanner is tested under most favourable conditions.

Table 1: Properties of the Water

Turbidity [NTU]	Temperature [° C]	Pressure [dBar]	Salinity [PSU]
0.00	20.582	0.097	0.279

The other measured parameters, being a water temperature of 20.582 °C, a water pressure of 0.097 dBar and a salinity of 0.279 PSU can be used to compute the density of the water. By applying the “UNESCO equation of state” for density in terms of salinity, temperature and pressure [Intergovernmental Oceanographic Commission, 2010] and entering the measured values at a water pressure of 0.097 dBar, an in-situ density of 998.292 kg/m³ is calculated. Overall, the density of water increases with a decreasing temperature, an increasing salinity or an increasing pressure whereas pressure has the smallest impact [Webb, 2023]. Since the measurements are conducted in a closed basin over a time period of 1.5 h, it is assumed that the properties of the water remain constant. Considering that this study focuses on the reflectivity behaviour of different materials, the intensity of the received signal is then predominantly influenced by the surface characteristics of the selected target materials.

During the test measurements, the settings summarized in the following Table 2, are used. Considering that ULi measures 100.000 points per second and skipping none of the pulses, a pulse rate of 100 kHz applies. By selecting the filter “adjustment”, the green laser is emitted with a strength corresponding to the lowest possible laser class 2M. Since the scanner is operated in a small acrylic glass basin, the green laser is reflected multiple times in an uncontrolled manner. Hence, the reduction of the laser power increases the safety of work in a laboratory environment. To test the reflectivity behaviour, a radius change speed of 0 Hz is used. By means of that, the laser rotates with a constant radius on the target surface. To scan the entire surface of targets, the radius change speed is adjusted to 0.01 Hz. In this case, the laser rotates with a firstly increasing and then decreasing radius and therewith captures the surface of the target including its holes, cracks and knotholes.

Tab. 2: Settings of ULi

Max distance [m in water]	5
Skip distance [m in water]	0
Skip pulses	0
Filter	adjustment
Laser pattern	Circle
Motor speed [Hz]	5
Radius change speed [Hz]	0
Radius	0.6

The incoming waveforms can be directly reviewed in real-time using the Raw Signal Monitor. As it can be seen in the illustrated example for a white acrylic target in the Figure 6 below, the live monitor displays three curves. The red curve refers to a fiber reference which is recorded before the light leaves the scanner. Thus, it functions as an internal reference signal. Once the light is transmitted and reflected, it reaches a detector where an avalanche photodiode converts the optical signal into an electrical signal. The electrical signal is split by a ratio of 1:10 between two amplifiers. Subsequently, the signal is strengthened to varying degrees. While the signal, which is attenuated by a factor of 10, is denoted as the sensitive channel and coloured in green, the other signal is denoted as rough or less sensitive channel and coloured in blue. Consequently, the green coloured signal is much more sensible and therefore well suited for the detection of targets in clear water at a close range.

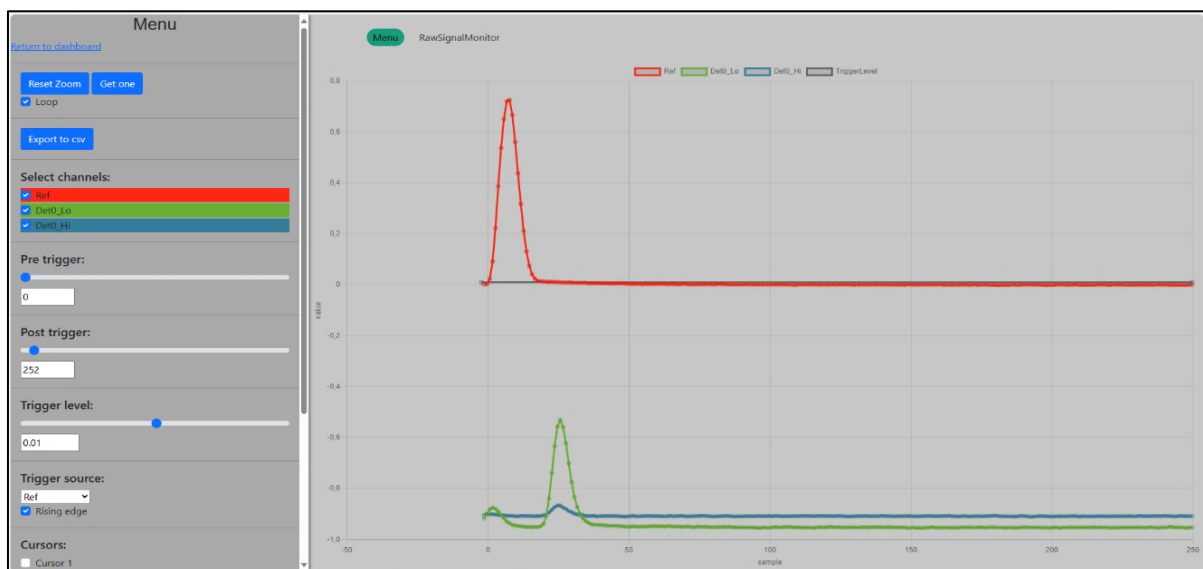


Fig. 6: Raw Signal Monitor for the white smooth acrylic plate target

In the illustrated example above, the first peak of the green coloured curve indicates the reflection of the green laser on the lenses of the scanning unit while the second peak refers to the reflection triggered from the target. To assess the distance between the lenses of the underwater laser scanner and the target, the number of samples between the first and the second peak is determined. Since each sample has a length of approximately 2.2 cm, the determined sample difference from the x-axis is multiplied with this length. For a rough estimation, the sample difference is directly derived from the raw signal monitor. In this case, the first peak occurs at 5 samples and the second at 25 samples, resulting in a sample difference of 20 samples. Multiplied with the sample length, the target is situated in a distance of about 44 cm. This distance is regarded as realistic.

6. POST PROCESSING AND RESULTS

After all test measurement are conducted, the acquired data is downloaded and post-processed. The retrieved waveforms are processed in Pulsalyzer, Python and CloudCompare.

Pulsalyzer is a proprietary post-processing software solution developed by the Fraunhofer IPM which can be used to review the derived waveforms, assess the associated point clouds and export the data. To assess the exact distance between the lenses of the underwater laser scanner and the target, the waveforms are further processed in Python. As previously outlined, the distance can be computed by multiplying the distance between the first two peaks with a sampling length of 2.2 cm. To ensure a clear identification of the two peaks, the waveform is filtered using the Savitzky-Golay-Filter. Since this filter preserves the shape of the peaks and causes less distortion, it is particular suitable for curved data such as waveforms. Since each scan contains several hundreds up to thousands of waveforms, the determined distances within each waveform are averaged by computing a mean value. As a result, the distance varies between 52.70 cm for the squared aluminium target to 59.87 cm for the black matt acrylic target plate. Considering that the first decimetres behind the scanner lenses are strongly subject to noise, where particular the diffusion of the light at the lenses decreases the signal-to-noise ratio, it is evident that the measurements are conducted in the very near field. To further assess the quality of the data obtained from those near-field measurements, the in Pulsalyzer internally computed point clouds are exported as .las files. These .las files are imported into the open-source software CloudCompare. The point clouds for the first two materials, being the black and the white acrylic targets with differing surface characteristics, are shown in the following Figure 7.

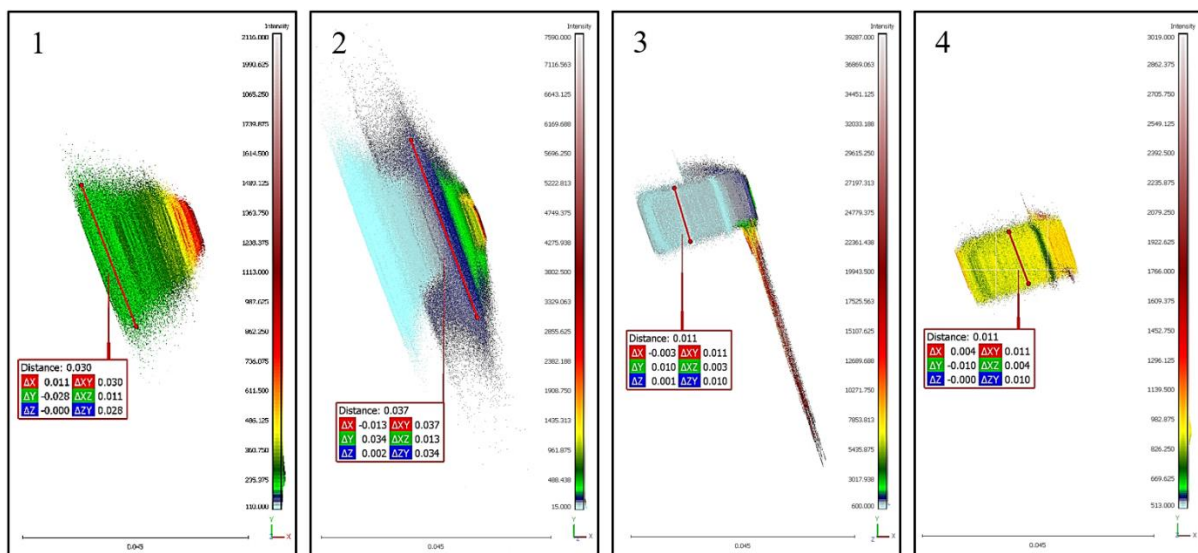


Fig. 7: Black Acryl matt [1], Black Acryl shiny [2], White Acryl smooth [3], White Acryl rough [4]

Since the underwater laser scanner does not deliver RGB colour information, the point clouds are coloured in accordance to their intensity values. Colouring by intensity does not only enable a better contrast and thus enhances the interpretation of the data, but it also allows to distinguish between the tested materials and their surface features. As it can be seen in the Figure 7, the intensity scale between the first two evaluated materials, greatly differs. While the intensity scale for the matt black surface reaches from 110.000 to 2116.000, covering a range of 2006 the scale for the shiny black surface reaches from 15.000 to 7590.000 and thus covers a much larger range of 7575. Subsequently, the shiny surface does not only evoke an overall higher maximum intensity, but it also causes a larger variation of intensity values. Meanwhile, the order and the range of the intensity values for the smooth white acrylic surface target is 10 times higher compared to the black acrylic surface and the white acrylic rough surface. However, as it can be seen from the side view, the high intensity values are attributed to reflections which do not belong to the target itself and which can therefore be considered as outliers. To further assess how well the emitted green laser reflects on both surfaces, the average maximum depth of the point cloud is measured with the Point picking tool. The measured distance indicates the redistribution of the laser light when it hits the object surface and therefore expresses the scattering. While the point cloud derived from the black acrylic matt target has an average maximum depth of 30 mm, the point cloud of the black acrylic shiny target has an average maximum depth of 37 mm. Consequently, the matt surface causes less scattering than the shiny surface. The mean width of the point cloud derived from the white acrylic smooth and rough surface is in each case 11 mm and hence much smaller in comparison to the black acrylic target. It is evident that variations in surface smoothness and roughness have little influence on the reflectivity behaviour. A rough surface is a surface for which the roughness exceeds the wavelength. In this case the light is scattered in different directions and a diffuse reflection occurs [Wolff, 2025]. Since the white acrylic plate was roughened using sandpaper, its roughness could not be numerically quantified, making it impossible to establish a direct relationship with the 532 nm wavelength. To put the obtained results in relation to the other tested materials, the materials and the measured width of the associated point cloud is visualized in the Figure 8. The x-axis indicates the target material and the y-axis the measured depth of the point cloud in millimetres, indicating the scattering. Since the measured distances are sorted in ascending order, it becomes evident that light, shiny and smooth surfaces are less subject to scattering than dark, matt and rough surfaces. That light surfaces are less subject to scattering and offer a better reflectivity can be attributed to the fact that white has a lower absorption coefficient, meaning that a white surface absorbs almost no light, but reflects it back. Furthermore, a smooth surface reflects the laser light in a directed matter while a rough or diffuse surface attenuates the signal and irregularly scatters it. Moreover, shiny, polished or metallic surfaces reflect light stronger in a certain direction, which is known as directional reflection. However, even if the reflectivity is high, the returning light beam is highly angle-dependent. The highest reflection is achieved at a perpendicular angle of incidence. If the receiver is not exactly positioned in the reflection angle, the laser beam can be reflected away which results in a loss of the signal. Nonetheless, since the green laser is transmitted almost horizontally, the angles of incidence and reflection are assumed to be similar. This results in a very high reflection, particularly on shiny and metallic surfaces. This overall reflection

behaviour is already known from terrestrial laser scanners. Hence, Vosselman and Maas [2010] state that the reflectivity of materials is wavelength dependent and that the strength of a pulse echo varies from close to 0 % for black rubber or coal dust to nearly 100 % for snow in the visibly wavelength range. Buksch and Lindenbergh [2007] go further and state that the scanning of dark surfaces is only reasonable reliable when using a scan angle of 0 ° and that the scanning of black and dark surfaces should generally be avoided.

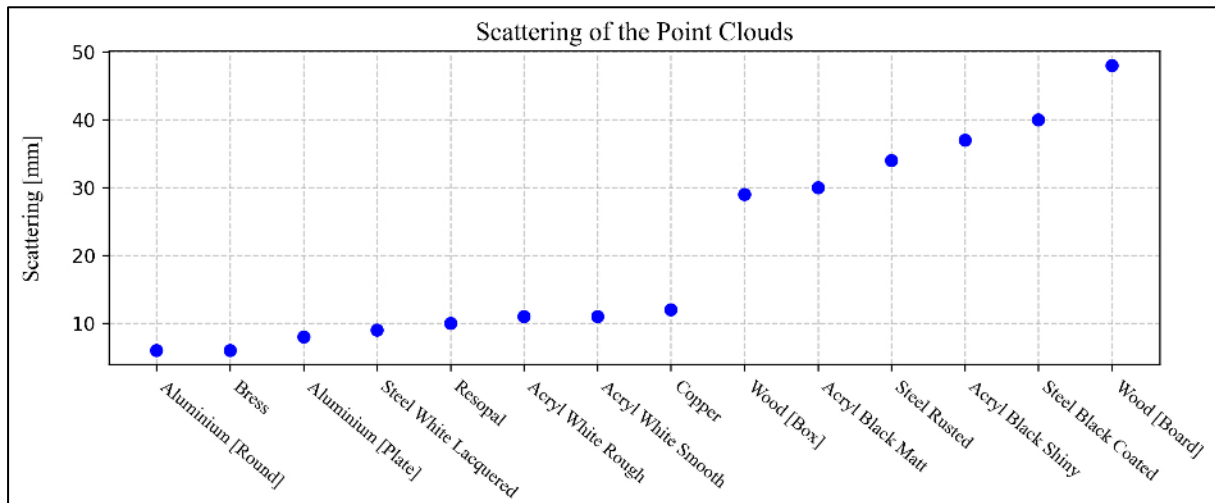


Fig. 8: Scattering of the tested materials in mm

To assess whether and to which extend the underwater laser scanner is able detect structures in the range of millimetres and can thus theoretically be used for inspection, maintenance and repair operations in the scope of monitoring tasks, the spiral scans are evaluated. As mentioned in the chapter 5. DATA ACQUISITION, the spiral is realized by setting the radius change speed to 0.01 Hz. Since the water in the test basin is only 0.454 m deep, the increasing radius causes the green laser to reach the surface of the water where it is additionally reflected. This reflection on the water surface is shown by the horizontal line in the Figure 9 [1,3,4,5,6] below. Subsequently, the circular pattern below this line shows the reflection of the real target whereas the pattern above the horizontal line represents the mirrored reflection on the waterline. As it can be seen from the reflection of the real target, the underwater laser scanner is able to capture holes and structures of various sizes. For the round aluminium target, offering the best reflectivity behaviour and the least scattering as outlined in the Figure 8, the two lateral holes are clearly captured by the scanner. To determine the actual size of those two holes, a digital calliper with a stated resolution of 0.01 mm is used. The size of each hole is measured to be 4.90 mm. Consequently, the underwater laser scanner is able to capture at least structures with a diameter in the range of millimetres. This also becomes present when evaluating the point cloud of the aluminium plate. As described in the chapter 4. TARGETS, the target has a total of 132 holes. When measuring the diameter of the holes with the digital calliper it becomes present, that the holes have different sizes. While the holes in the lower and upper left corner have a diameter of 5.00 mm, the hole in the upper right corner has a diameter of 5.16 mm.

Subsequently, the diameter of the holes deviates at a submillimetre scale. Nevertheless, all holes are captured by the underwater laser scanner. Concurrently, the white lacquered steel plate has holes with a diameter ranging from 5.20 mm in the lower right corner to 6.09 mm on the middle left side. In this case, not only the holes with the different diameters, but also the lettering in the upper centre of the target, just below the water surface, indicating “Mitsubishi xL 30U” is partly captured. As it can be seen in the Figure 5, the writing is done with a dark blue pen. Since dark colours have a higher absorption, the intensity of the reflected signal is also weaker. As it can be seen in the Figure 9, the lettering appears in a grey colour, referring to an intensity of about 400 when using the intensity indicator from the Point picking tool.

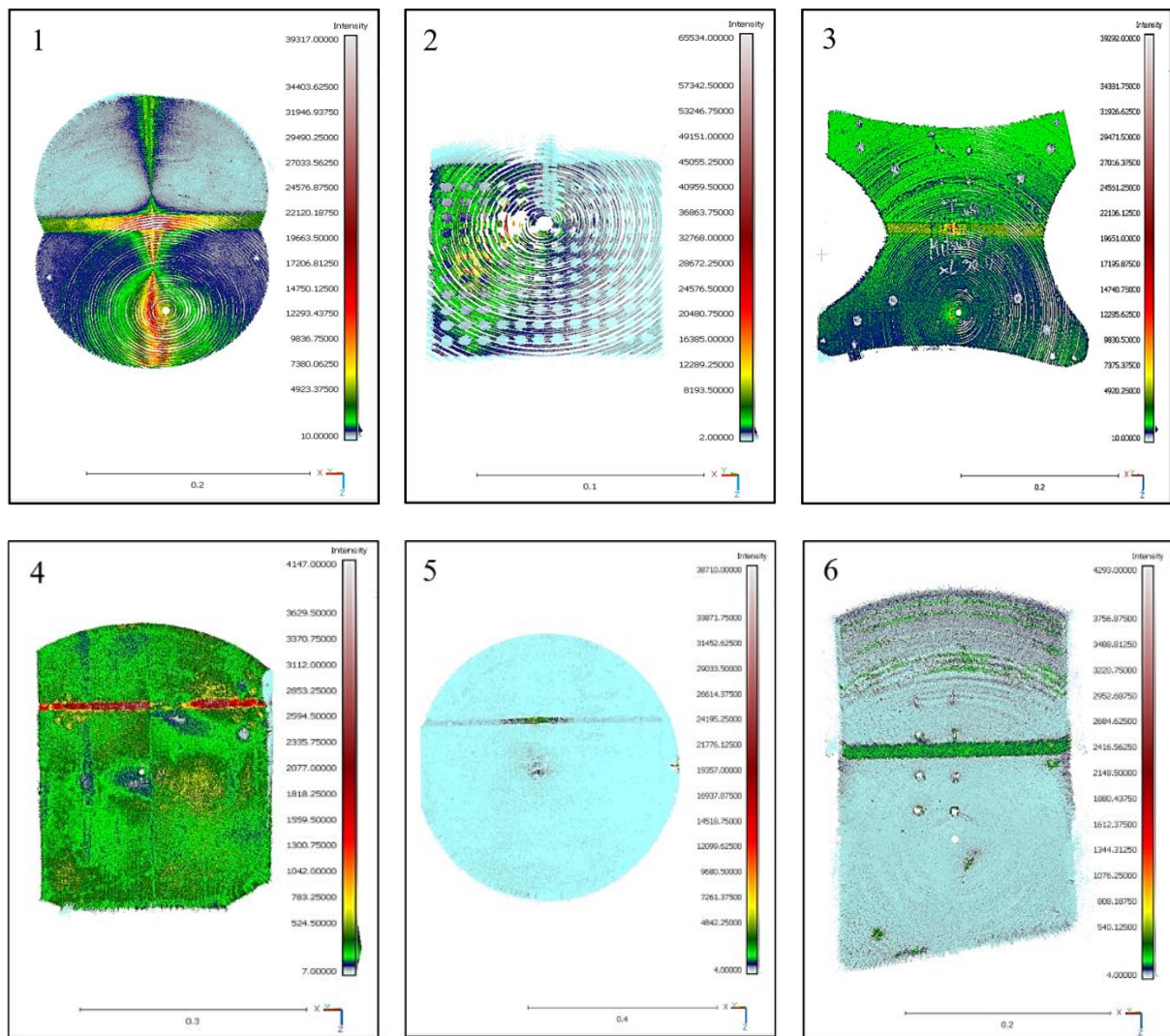


Fig. 9: Point Clouds retrieved from a Spiral Scan for the following targets: Aluminium Round [1], Aluminium Plate with holes [2], Steel White Lacquered [3], Wood [Box] [4], Steel Rusted [5] and Steel Black Coated [6]

For organic structures such as the illustrated point cloud from the wooden box, elements as the knotholes are mainly recognized because of the intensity difference. Since the knotholes and grains are comparably dark and clearly stand out from the actual light brown colour of the target, the lower reflectivity behaviour causes the intensity to decrease from green to dark blue. Meanwhile, the yellow coloured area on the right side beneath the two dark blue coloured knotholes indicates an increasing intensity. This can be attributed to the fact that this area is comparably clean and that the wood is not contaminated by black dirt. In addition to the good recognition of the knotholes, the 30 cm long and 2.36 mm wide vertical notch in the centre of the target is well identified. Contrary to that, the present grains are not well visible. Although there are some vertical lines, which are especially present on the lower half of the target, the annual rings cannot be continuously detected across the target. Hence, their visibility mainly depends on the contrast. The darker the grain or the annual ring in relation to the surrounding wood, the higher the contrast and the better the detectability. Subsequently, the underwater laser scanner cannot only detect well defined man-made geometrical objects such as holes, but also organic structures. To which extend the respective elements are identified is also driven by the material itself. This becomes present when reviewing the point cloud of the rusted steel plate. As already shown in the Figure 8, the respective point cloud has a depth of 34 mm. Hence, the rust layer causes a lot of scattering, resulting in an overall weak intensity of the reflected signal. Subsequently, the point cloud is nearly all over coloured in light blue, indicating an average intensity of 60. Following, only the outline of the two holes in the upper left and right corner, having a diameter of 6.86 mm and 9.80 mm respectively, are identified. The remaining holes are not covered by the spiral scan and can therefore not be compared. In a similar behaviour, the black coated steel target only causes a weak intensity of the reflected signal. Nevertheless, the four holes in the centre as well as the holes in the corners are clearly visible. Although the diameter of the holes in the centre, reaching from 6.59 mm to 6.71 mm are smaller compared to the ones of the rusted steel plate, the surface is smooth and not rough which can be the reason why the holes are recognized and identified to a greater extent. Overall, the selection of the targets shows, that the underwater laser scanner is able to detect targets with different shapes. Consequently, the quality of the derived point cloud, especially with regard to the captured edges and corners, is comparable. This holds true regardless of whether round targets such as the aluminium plate, squared targets like the wooden box, or irregular targets such as white lacquered steel plates are used.

7. CONCLUSION AND OUTLOOK

The research shows, that the quality of the point clouds derived from the underwater laser scanner ULi is not driven by the shape, but, predictably, to a great extent by the surface characteristics of the target. Hereby, two main factors, being the roughness and the surface finish, i.e. the matt and shininess, have been taken into consideration. The investigation of 14 selected materials shows, that light coloured targets with a shiny smooth surface offer an overall better reflectivity and cause less scattering compared to dark coloured, matt and rough surfaces. The scattering of the point clouds, reaching from 6 mm for the round aluminium target to 48 mm for the wooden plate target, is generally very high and clearly exceeds to what can be

derived from terrestrial laser scanners. This might be related to the fact that the measurements are conducted in the very near field, where the maximum distance between the lenses of the scanning unit and the target is 59.87 cm. Besides, the targets are not properly fixed. Holding the target by hand against the water pressure may have caused millimetre-scale fluctuations, leading to an increased scattering in the point clouds. Nevertheless, the investigation shows, that the point clouds derived from this particular underwater laser scanner can be used to identify man-made structures such as drilled holes or cracks as well as organic structures down to the millimetre scale. To verify the statement of the manufacturer, saying that measurements carried out in clear water offer a submillimetre precision, further measurements with sophisticated ground truth measurements are required. For this purpose, the target objects should also be scanned by high accurate terrestrial instruments when being out of the water to compare the retrieved point clouds with each other. Another option would be to develop and establish structures, such as a Böhler-Star to assess the achievable resolution [Böhler et al., n.d.]. Furthermore, test measurements with varying distances between the scanning unit and the target itself have to be carried out. This should not only involve static, but also dynamic measures to evaluate the suitability of integrating ULi on underwater vehicles. As the achievable precision and range strongly depends on the quality of the water body, further investigations and studies in water bodies offering different levels of turbidity are crucial. Subsequently, the degree of precision which can be achieved in other, more turbid, real world environments, must be investigated. This is especially relevant when evaluating the application of ULi for monitoring tasks in harbour environments, where the shipping traffic additionally pollutes the water. Similar, the suitability of ULi for offshore practices, where not only the salinity in the water increases but also where suspended particles and currents contribute to a higher level of turbidity, must be tested in respective environments.

Consequently, the presented research can be considered as a first assessment which shows, that the point clouds derived from ULi can be used to identify man-made and organic structures in the range of millimetres. To estimate the ultimate minimum magnitude at which those structures can still be detected, further studies and the inclusion of sophisticated reference data functioning as ground truth, are essential. Besides, further research in additional real-world environments such as rivers, lakes or oceans, offering varying levels of turbidity, are required. Respective investigations would not only help to derive a more sophisticated statement about the achievable precision, but would also help to narrow down possible fields of application for ULi. Hence, such additional studies will help to assess whether ULi can be considered as the fast, precise and high-resolved monitoring solution the worldwide expansion of underwater infrastructure elements requires.

REFERENCES

Buksch, A., Lindenbergh, R. (2007): Error budget of terrestrial laserscanning: influence of the intensity remission on the scan quality. Conference paper for the 3 International Scientific Congress Geo-Siberia. P. 6, 12. Novosibirsk, Russia.

Böhler, W., Vident, M., Marbs, A. (n.d.): Investigating Laser Scanner Accuracy.

Fraunhofer IPM (2024): Underwater LiDAR System. Optical inspection of underwater infrastructure. Long range, high precision 3D mapping.

Hildebrandt, M., Kerdels, J., Albiez, J., Kirchner, F. (2008): A practical underwater 3D-Laserscanner. Conference paper for the OCEANS Conference. PP. 1-5. Canada.

Intergovernmental Oceanographic Commission (2010): The international thermodynamic equation of seawater - 2010. Calculation and use of thermodynamic properties. Manuals and Guides 56. P. 18. UNESCO.

Nauert, F., Kampmann, P. (2023): Inspection and maintenance of industrial infrastructure with autonomous underwater robots. *Front.Robot.AI Sec. Field Robotics*. Volume 10. P. 1. Frontiers.

Shan, J., Toth, C.K. (2018): *Topographic Laser Ranging and Scanning. Principles and Processing*, Second Edition. P. 1. CRC Press.

Vosselman, G, Maas, H-G. (2010): *Airborne and Terrestrial Laser Scanning*. P. ix and P.15. Whittles Publishing Ltd. Scotland.

Webb, P. (2023): *Introduction to Oceanography*. Chapter 6.3 Density. P. 1. Roger Williams University.

Wolff, C. (2025): Reflection at smooth surfaces. P. 1. Radartutorial.

Witte, B., Sparla, P. (2015): *Vermessungskunde und Grundlagen der Statistik für das Bauwesen*. P. 208. Wichmann Verlag. Berlin.

BIOGRAPHICAL NOTES

M. Sc. Annika L. Walter works as a research associate in the department Hydrography and Geodesy of the HafenCity University since 2023. She obtained her Master of Science in Geodesy and Geoinformatics with a Specialization in Hydrography in 2023. She is involved into teaching and research. Ms. Walter is a member of the DVW as well as of the DHyG.

M. Sc. Ellen Heffner works as a research associate in the department Hydrography and Geodesy of the HafenCity University since 2022. She obtained her Master of Science in Geodesy and Geoinformatics with a Specialization in Hydrography in 2022. She is involved into teaching and research. Mrs. Heffner is a member of the DVW as well as of the DHyG.

Dr.-Ing. Annette Scheider is the head of the geodetic laboratory at the HafenCity University Hamburg since 2018. Between 2010 and 2018 she was a research associate at University of Stuttgart. She is a member of the DVW, as well as the DVW working group 8 (Mobile and Autonomous Sensor Systems) and the DHyG.

Prof. Dr.-Ing. Harald Sternberg is professor for Hydrography and Geodesy at the HafenCity University Hamburg since 2017. Prior to that, he served as a Professor of Engineering Geodesy and Geodetic Metrology since 2001 and spent 13 years as Vice President for Teaching and Studies at the HafenCity University Hamburg. Mr. Sternberg conducts research in the fields of hydrography, indoor navigation and data-driven analysis. He is a member of the DVW (where he chaired the Multi-Sensor-Systems working group in the past) and of the DHyG. Moreover, Mr. Sternberg was delegated to the IBSC (FIG/IHO/ICA international board on standards of competence for hydrographic surveyors and nautical cartographers) by the FIG.

CONTACTS

M. Sc. Annika L. Walter, M. Sc. Ellen Heffner, Dr.-Ing. Annette Scheider and Prof. Dr.-Ing. Harald Sternberg
HafenCity University Hamburg
Henning-Voscherau-Platz 1
20457 Hamburg
GERMANY
Tel. +49 40 42827 5511
Email: annika.walter@hcu-hamburg.de, ellen.heffner@hcu-hamburg.de, annette.scheider@hcu-hamburg.de and harald.sternberg@hcu-hamburg.de